



Original Research

miR-22 exerts anti-alzheimic effects via the regulation of apoptosis of hippocampal neurons

Yu Wang, Lan Zhao, Bohong Kan, Huiyan Shi, Jingxian Han*

Department of Acupuncture and Moxibustion, First Teaching Hospital of Tianjin University of Traditional Chinese Medicine, Tianjin, China

Correspondence to: dr1308@163.com

Received October 16, 2018; Accepted December 22, 2018; Published December 31, 2018

Doi: <http://dx.doi.org/10.14715/cmb/2017.64.15.14>

Copyright: © 2018 by the C.M.B. Association. All rights reserved.

Abstract: To investigate the expression of miR-22 in the hippocampus of amyloid β (1-42)-induced alzheimeric rats, and to assess the underlying mechanism. A total of 60 male Sprague Dawley rats weighing between 274.65 and 293.97 g (mean weight = 284.31 \pm 9.66 g) and aged 12 to 14 weeks were randomly assigned to three groups: control group (n = 20), Alzheimer's disease group (AD group; n = 20) and AD + miR-22 mimic group (ADMM group; n = 22). Rat AD model was established by injecting a solution of A β 1-42 into the hippocampal CA1 regions. After 24 h, rats in the ADMM group also received intraventricular injection of miR-22 mimic continuously for 28 days. The escape latency of rats, neuronal damage in the hippocampus, synaptic structure, brain-derived neurotrophic factor (BDNF), and the expressions of apoptosis-related proteins were assessed or determined, as appropriate. The expression of miR-22 in hippocampus of the AD group was significantly lower than that in the control group ($p < 0.05$). However, after 28 days of intraventricular injection of miR-22 mimic into AD rats, the expression was significantly increased, relative to control ($p < 0.05$). The escape latency of AD rats was significantly prolonged, and the number of platform sites significantly reduced when compared to the control group ($p < 0.05$). However, the escape latency was significantly shortened and the number of platform sites significantly increased in the ADMM group, relative to the control and AD groups. Results of transmission electron microscopy showed that the expression of miR-22 significantly reversed the degradation of synaptic structures in the hippocampus of AD rats as evidenced by recovery of abnormal synaptic cleft width and the length of synaptic active zones ($p < 0.05$). Results of Nissl staining revealed significant proliferation of gliocyte and loss of Nissl bodies. After miR-22 injection, the number of gliocytes in the hippocampus of AD rats was significantly reduced, while the number of Nissl bodies was significantly increased ($p < 0.05$). The expressions of BDNF in CA1 and CA2/3 regions of AD rats were significantly lower than those in the control group, and BDNF in the hippocampus of AD rats was significantly increased after 28 days of continuous injection of miR-22 ($p < 0.05$). The positive expression of Tunnel in the ADMM group (22.67 \pm 2.96 %) was significantly higher than that in the AD group (4.49 \pm 1.23 %), but significantly lower than that of control (39.51 \pm 3.66 %) ($p < 0.05$). After 28 days of intraventricular injection of miR-22 mimic into AD rats, the expression of Bax protein was significantly down-regulated, while bcl-2 protein was significantly up-regulated ($p < 0.05$). The expression of miR-22 in the hippocampus of patients with AD inhibits neuronal apoptosis, thereby improving learning and memory dysfunction.

Key words: MiR-22; Alzheimer's disease; Hippocampal neurons; Apoptosis; Expression.

Introduction

Alzheimer's disease (AD), the most common neurodegenerative disease in the elderly, is a major cause of dementia, and it is characterized by memory loss and cognitive decline (1). Amyloid beta peptide (A β) which is deposited and accumulated within the brain tissues of patients with AD affects the structure and function of synapses via disruption of the synaptic signaling pathway, leading to complete loss of synaptic function (2). Neuronal apoptosis and formation of neurofibrillary tangles are also important pathological changes in the pathogenesis of AD, and apoptosis of neurons may be responsible for their death (3, 4). These pathological changes give rise to impaired memory and activity in patients with AD. The occurrence and development of AD are co-regulated by genetic and environmental factors (5). At present, little or nothing is known about the precise molecular mechanisms underlying the pathogenesis of AD.

MicroRNA (miRNA), a single stranded non-coding RNA in eukaryotes contains 20 to 24 nucleotides and exerts regulatory functions (6). Through binding to spe-

cific genes, miRNAs regulate the expressions of several genes, and thus play important roles in physiological activities such as cell proliferation, differentiation and apoptosis (7). For instance, the inhibition of miRNA-155 can significantly improve impaired neurologic function in rats with cerebral infarction, reduce the size of cerebral infarction, and effectively promote angiogenesis in the ischemic area, through the AT1R/VEGFR2 pathway (8). In a previous study, it was reported that miRNA-195 is a targeted inhibitor of vascular endothelial growth factor A (AEGF A), and that inhibition of its expression can significantly augment angiogenesis in the ischemic area (9). In AD models, the level of expression of miR-26b is significantly increased, and this can activate the phosphorylation of Tau protein, resulting in abnormal replication of DNA and excessive neuronal apoptosis (10). In Huntington's disease, miR-22 restrains the progression of the disease via the inhibition of neuronal apoptosis. It binds to mRNA of virulence genes such as HDAC4, Rcor1 and Rgs2 thereby alleviating severity of the disease (11). The aim of this study was to investigate the expression of miR-22 in hippocampus of amyloid β (1-42)-induced alzheimeric rats, and

to assess the underlying mechanism.

Materials and Methods

Rats and preparation of β -amyloid peptide solution

A total of 60 male Sprague Dawley rats weighing between 274.65 and 293.97 g (mean weight = 284.31 ± 9.66 g) and aged 12 to 14 weeks were randomly assigned to three groups: control group ($n = 20$), Alzheimer's disease group (AD group; $n = 20$) and AD + miR-22 mimic group (ADMM group; $n = 22$). There were no significant differences in general data such as age and body weight among the three groups. A solution of A β 1–42 was prepared by dissolving the white powder-like crystals in isopropanol at room temperature overnight. The isopropanol was eventually evaporated using a gentle stream of nitrogen, and the peptide obtained was re-dissolved in dimethyl sulfoxide (DMSO) and made to a final concentration of 1 mg/ml and stored in a -20 °C refrigerator. After 48 h of refrigeration, the solution was diluted to 2 μ g/ μ l with phosphate-buffered saline (PBS).

Establishment of AD rat model

The rats were anesthetized using 10 % chloral hydrate (4 ml/kg body weight, b.wt.) and the solution of A β 1–42 peptide (5 μ l) was injected into their lateral ventricles from a site 1.1 mm behind the anterior iliac crest, 2.2 mm lateral to sagittal plane and 3.0 mm below dura mater using a micro-injector.

Morris water maze (MWM) test

The praxiological information of rats in the water maze was collected using ANY-maze video acquisition system. The rats were introduced into the pool at one of the four entries and different entries were used in a day. They were given 60 sec to find the site of the platform, and once they did, they remained there for another 10 sec. Those that could not find the platform within 60 sec, were put on it for 10 sec, and thereafter taken out of the pool. The escape latency of rats from water to searching and climbing on the platform (an index reflecting memory ability) was observed and recorded.

Determination of ultrastructure

Brain tissues from the rats were cut into two parts and further sliced into bits (100 μ m) using a refrigerated microtome after an initial fixation with 2.5 % glutaraldehyde. The samples were fixed, dehydrated, soaked and embedded using different gradients of acetone. The embedded sections were double-stained with uranyl acetate and lead citrate. The middle third of the CA1 layer of the hippocampus was observed using transmission electron microscopy, and the number of synapses, the width of synaptic gap and length of synaptic activity area in the hippocampus of each group were quantified.

Nissl Staining

The hippocampus tissues of the rats were dipped in a 30 % sucrose solution and sliced under freeze into bits (30 μ m). The slices were immobilized on glass slides pretreated with gelatin and air-dried. They were subsequently stained with tar purple at 37 °C within 30 min and thereafter subjected to color separation and dehydration using a gradient of ethanol concentration, and

then sealed after xylene treatment. Photomicrographs of the slides were viewed under a light microscope.

Immunohistochemical staining (SP Method)

The brain sections were heated in a 60 °C oven for 30 min and dewaxed with xylene thrice within 5 min and dehydrated thrice using 100, 95, and 79 % ethanol per procedure. Endogenous activity of peroxidase was inhibited using a mixed solution of methanol and 3 % hydrogen peroxide, and finally sealed with goat serum within 1 h. Anti-BDNF antibodies were diluted 1:200, incubated overnight at 4 °C, and then washed 4 times with PBS on a shaker. After the addition of secondary antibody, diaminobenzidine (DAB) was added for color development, after which 6 samples were randomly selected from each group, and 5 fields of view were chosen for each sample for photographing under a light microscope ($\times 400$).

Real-time polymerase chain reaction (RT-PCR)

Total RNA was extracted from hippocampus tissue using Trizol reagent and its concentration and purity determined spectrophotometrically at wavelengths of 260 and 280 nm. The mRNA was converted to cDNA via reverse transcription and then refrigerated at -80 °C. The RT-PCR system consisted of buffer (2.5 μ l), cDNA (2 μ l), 0.25 μ l of 20 μ mol/l forward primer, 0.25 μ l of 20 μ mol/l reverse primer, 0.5 μ l dNTPs (10 mmol/l), 0.5 μ l Taq polymerase (106 U/l), and 19 μ l ddH₂O. The amplification systems for RT-PCR were identical.

Tunnel staining procedure

The brain sections were heated in a 60 °C oven for 30 min, dewaxed thrice using xylene within 5 min, and dehydrated thrice using 100, 95, and 79 % ethanol per procedure. They were incubated with proteinase k for 30 min, and rinsed with PBS, after which terminal deoxyribonucleotidyl transferase (TdT) and luciferase-labeled dUTP were added and the reaction mixture was incubated at 37 °C for 1 h. This was followed by the addition of horseradish peroxidase-labelled specific antibody and incubation at 37 °C for another 1 h, after which DAB reagent was used as a substrate, and the reaction was allowed to proceed at room temperature for 10 min. Immediately following hematoxylin staining, photomicrographs of the slides were taken and viewed under a light microscope.

Western blotting

Brain tissues from the rats were completely ground in ice-cold radio-immunoprecipitation assay buffer (RIPA) and ultrasonically decomposed. The lysate was centrifuged at 3000 rpm for 10 min and the aspirated supernatant dispensed into Eppendorf tubes. Protein concentration was measured spectrophotometrically based on the BCA method and the dispensed samples refrigerated at -80 °C. Protein separation was achieved with sodium dodecyl sulfate-polyacrylamide gel electrophoresis (SDS-PAGE) and the bands transferred to PVDF membranes within 35 min. Membranes with target proteins were blocked with 5 % skim milk powder at 37 °C, and incubated with primary antibodies at 4 °C overnight, followed by incubation with goat anti-rabbit secondary antibody for 1 h in the dark. The protein

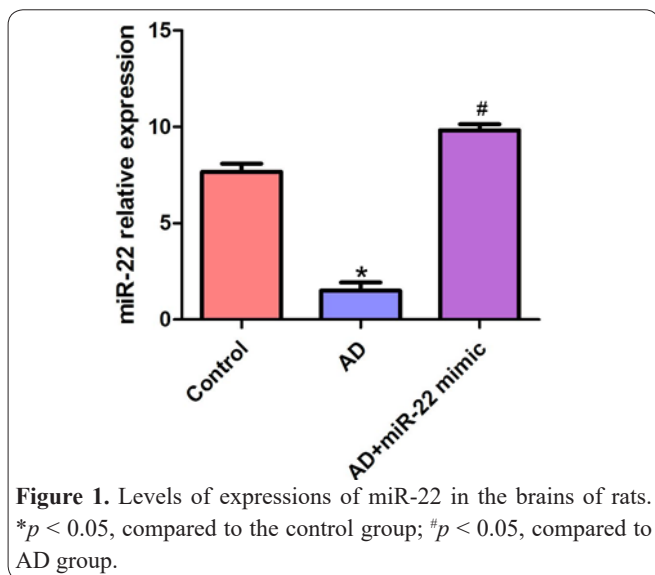


Figure 1. Levels of expressions of miR-22 in the brains of rats. * $p < 0.05$, compared to the control group; # $p < 0.05$, compared to AD group.

bands were scanned and quantified using an Odyssey membrane sweeper. Glyceraldehyde 3-phosphate dehydrogenase (GAPDH) was used as internal control.

Statistical analysis

Measurement data are expressed as mean \pm SD and the statistical analysis was performed using SPSS (22.0). Groups were compared using Student *t*-test and values of $p < 0.05$ were considered statistically significant.

Results

Expressions of miR-22 in the brain tissues

The expression of miR-22 in hippocampus of the AD group was significantly lower than in that the control group ($p < 0.05$). However, after 28 days of intraventricular injection of miR-22 mimic into AD rats, the expression was significantly increased relative to control ($p < 0.05$; Figure 1).

Outcomes of the Morris water maze test

The escape latency of AD rats was significantly prolonged and the number of platform sites significantly reduced, when compared to the control group ($p < 0.05$). However, the escape latency was significantly shortened and the number of platform sites significantly increased in the ADMM group, compared to control and AD groups ($p < 0.05$; Figure 2).

Effect of the expression of miR-22 on synaptic structures

Results of transmission electron microscopy showed that the expression of miR-22 significantly reversed the degradation of synaptic structures in the hippocampus of AD rats as evidenced by the recovering of abnormal synaptic cleft width and the length of synaptic active zones ($p < 0.05$). These results are shown in Figure 3.

Effect of miR-22 on morphology of the hippocampus of AD rats

Results of Nissl staining revealed significant proliferation of gliocyte and loss of Nissl bodies. After miR-22 injection, the number of gliocytes in the hippocampus of AD rats was significantly reduced, while the number of Nissl bodies was significantly increased ($p < 0.05$;

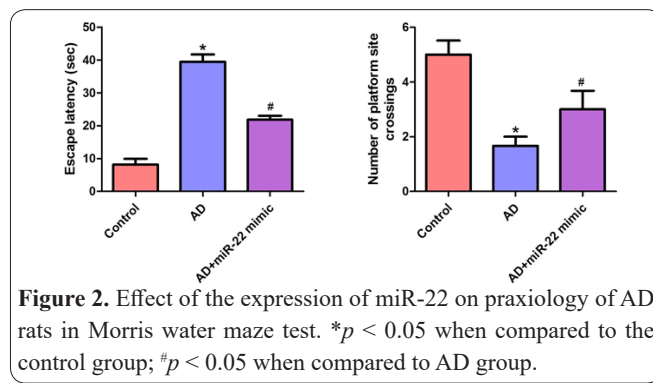


Figure 2. Effect of the expression of miR-22 on praxiology of AD rats in Morris water maze test. * $p < 0.05$ when compared to the control group; # $p < 0.05$ when compared to AD group.

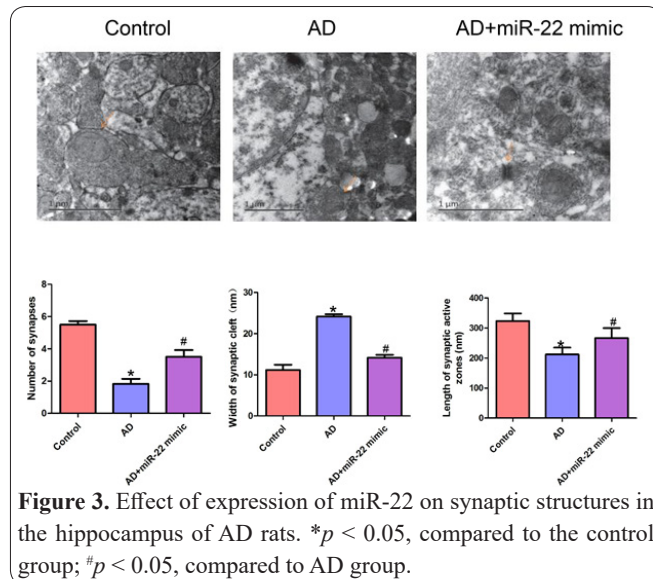


Figure 3. Effect of expression of miR-22 on synaptic structures in the hippocampus of AD rats. * $p < 0.05$, compared to the control group; # $p < 0.05$, compared to AD group.

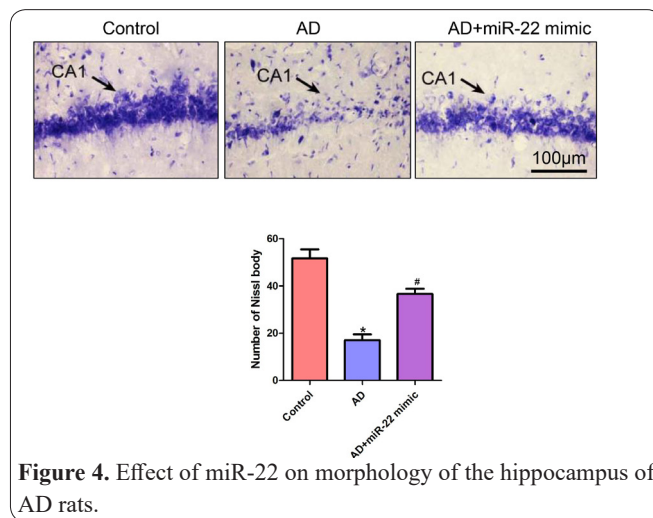


Figure 4. Effect of miR-22 on morphology of the hippocampus of AD rats.

Figure 4).

Effect of miR-22 on BDNF in the hippocampus of AD rats

The expressions of BDNF in CA1 and CA2/3 regions of AD rats were significantly lower than those in the control group, and BDNF in the hippocampus of AD rats was significantly increased after 28 days of continuous injection of miR-22 ($p < 0.05$; Figure 5).

Effect of miR-22 on Tunnel of neurons in the hippocampus of AD rats

As shown in Figure 6, the positive expression of Tunnel in the ADMM group ($22.67 \pm 2.96\%$) was significantly higher than that in the control group ($4.49 \pm 1.23\%$), but significantly lower than that in the AD

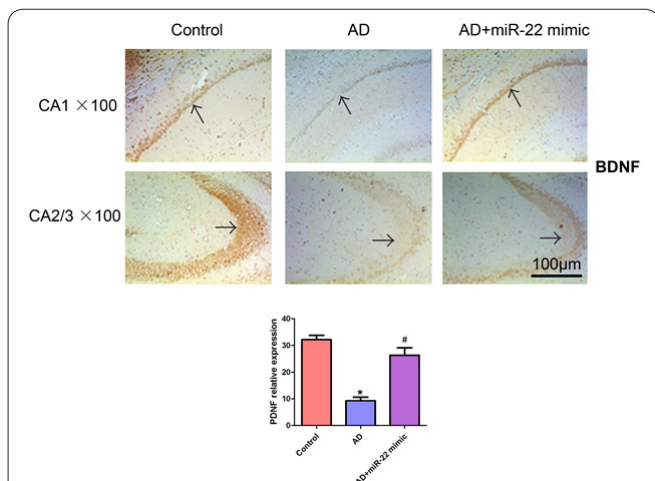


Figure 5. Effect of miR-22 on BDNF in the hippocampus of AD rats. CA1: hippocampus zone 1; CA2/3: hippocampus zone 2/3; brown color indicated with an arrow = positive result. * $p < 0.05$, compared to the control group; # $p < 0.05$, compared to AD group.

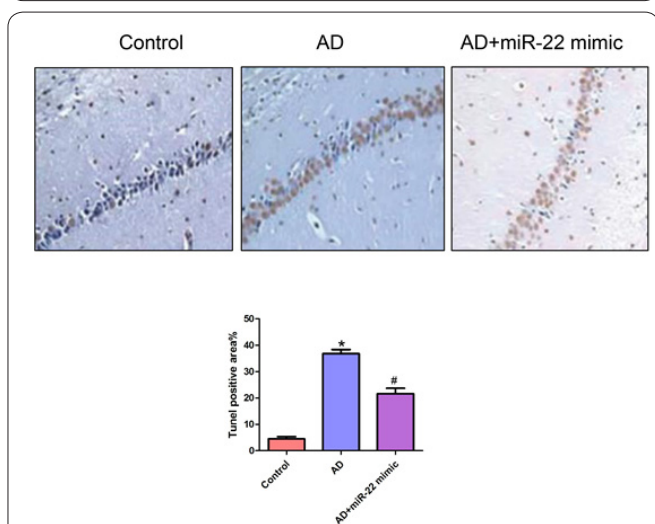


Figure 6. Effect of miR-22 on TUNEL of neurons in the hippocampus of AD rats. * $p < 0.05$, compared to the control group; # $p < 0.05$, compared to AD group.

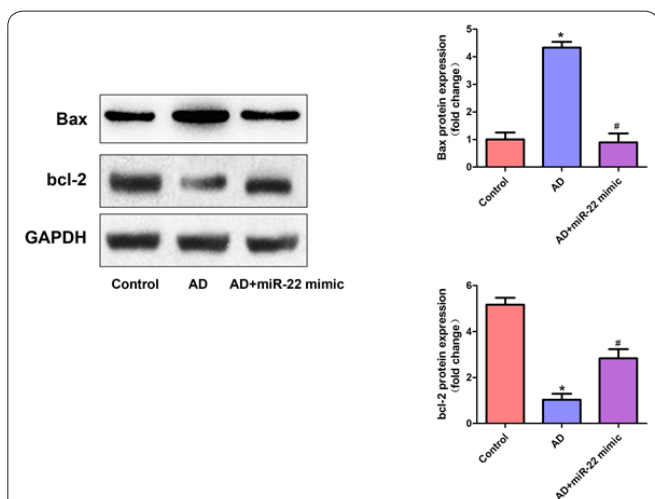


Figure 7. Effect of miR-22 on the expression of apoptosis-related neuronal genes in the hippocampus of AD rats. * $p < 0.05$, compared to the control group; # $p < 0.05$, compared to AD group.

group ($39.51 \pm 3.66\%$) ($p < 0.05$).

Effect of miR-22 on the expressions of apoptosis-related neuronal genes in the hippocampus of AD rats
After 28 days of intraventricular injection of miR-22

mimic into AD rats, the expression of Bax protein was significantly down-regulated while that of bcl-2 protein was significantly up-regulated ($p < 0.05$; Figure 7).

Discussion

Alzheimer’s disease (AD) is a typical neurodegenerative disease characterized by cognitive decline and memory loss (12). The World Health Organization (WHO) has predicted that the number of patients with AD in Europe and United States will rise to 30 million by 2050 (13). In China only, there are approximately 6 million AD patients, accounting for one-third of the world’s total and the number grows at a rate of 18,000 persons per annum, thereby creating a huge burden on a patients’ families and society (14, 15). This disease has been rated the fourth common chronic disorder in the elderly, and is closely followed by cardiovascular diseases, stroke and cancer (16). Oxidative stress, inflammation, β -starch cascades, gene mutations and apoptosis of neurons are important causes of AD (17). However, the precise molecular mechanism underlying its pathogenesis is not well understood.

Cell apoptosis refers to programmed cell death controlled by genes in order to maintain homeostasis under physiological or pathological conditions (18). In a previous study, it was reported that a large number of neurons in the brain tissues of patients with AD exhibit a new type of cell cycle, and they may be easily lost, thereby further aggravating the formation of neurofibrillary tangles (19). In addition, it is reported that glia-cytes in the hippocampus of patients with AD are abnormally increased, and that this results in the secretion of inflammatory cytokines such as interleukin-10 (IL-10) and tumor necrosis factor α (TNF- α) which enhance the toxicity of neurons via the induction of inflammatory cascades, leading to aggravation of neuronal apoptosis in the hippocampus of AD patients (20).

In the present study, the expression of miR-22 in hippocampus of the AD group was significantly lower than that in the control group. However, after 28 days of intraventricular injection of miR-22 mimic into AD rats, the expression was significantly increased relative to control.

As a member of miRNAs family, MiR-22 plays an important role in the pathogenesis of cancer, as well as cardiovascular and neurodegenerative diseases (21). It induces senility in tumor cells by targeting and inhibiting the expressions of aging-related genes such as CDK6, SIRT1 and Sp1, thereby inhibiting the development of tumors (22). However, in patients with myelodysplastic syndrome, the expression of miR-22 is abnormally elevated, and so it can advance the self-renew and transformation of hemopoietic stem cells by targeting and inhibiting the anti-oncogene “TET2”. The up-regulation of miR-22 promotes adipogenic differentiation of mesenchymal stem cells derived from human adipose tissue and osteogenic differentiation by restraining the expression of HDAC6 protein.

In this study, the escape latency of AD rats was significantly prolonged and the number of platform sites significantly reduced, when compared to the control group. However, the escape latency was significantly shortened and the number of platform sites significant-

ly increased in the ADMM group, when compared to control and AD groups. This result appears to suggest that miR-22 may be able to effectively improve learning and memory disorder in AD rats. Results of transmission electron microscopy showed that miR-22 significantly reversed the degradation of synaptic structures in the hippocampus of AD rats as revealed by recovering of abnormal synaptic cleft width and the length of synaptic active zones. Results of Nissl staining revealed significant proliferation of gliocyte and loss of Nissl bodies. After miR-22 injection, the number of gliocytes in the hippocampus of AD rats was significantly reduced, while the number of Nissl bodies was significantly increased.

Brain-derived neurotrophic factor (BDNF) promotes synaptic growth and conduction, and increases its plasticity. Therefore, its level can reflect the severity of degenerative nervous system disease to a certain extent. In this study, the expression of BDNF in CA1 and CA2/3 regions of AD rats were significantly lower than those in the control group, and BDNF in the hippocampus of rats was significantly increased after 28 days of continuous injection of miR-22. The positive expression of Tunnel in the ADMM group was significantly higher than that in the AD group, but significantly lower than that of control. This result suggests that the overexpression of miR-22 may significantly reduce neuronal apoptosis in the hippocampus of AD rats. After 28 days of intraventricular injection of miR-22 mimic into AD rats, the expression of Bax protein was significantly down-regulated, while bcl-2 protein was significantly up-regulated.

The likely limitations in this study are lack of data from *in vitro* experiments to support results obtained *in vivo*, and the non-inclusion of a direct target and signaling pathway of miR-22.

The results obtained in this study have shown that the expression of miR-22 in the hippocampus of patients with AD improves learning and memory dysfunction by inhibiting neuronal apoptosis.

Acknowledgements

Funded by National Natural Science Foundation of China 81704148 and Scientific Research Project of Tianjin Municipal Education Commission 2017KJ149.

Interest conflict

No competing interest is associated with this study.

Author contributions

Jingxian Han designed the research. Yu Wang, Lan Zhao, Bohong Kan, Huiyan Shi, Jingxian Han performed the cytotoxicity and reversal experiments. Yu Wang performed PCR and Western blot experiments. All authors analysed the results and took part in preparing the manuscript.

References

1. Jack CR, Bennett DA, Blennow K. NIA-AA Research Framework: Toward a biological definition of Alzheimer's disease. *Alzheimers Dement* 2018; 14: 535.
2. Alaa AM, Yoon J, Hu S, van der Schaar M. Personalized Risk Scoring for Critical Care Prognosis Using Mixtures of Gaussian Processes. *IEEE Trans Biomed Eng* 2018; 65: 207-218.

3. Harrison P. Alzheimer's disease and chromosome 14: Different gene, same process? *British J Psychiatr* 2018; 163: 2-5.
4. Cope TE, Rittman T, Borchert RJ, Jones PS, Vatansever D, Allinson K. Tau burden and the functional connectome in Alzheimer's disease and progressive supranuclear palsy. *Brain* 2018; 141: 550-567.
5. Idda ML, Munk R, Abdelmohsen K, Gorospe M. Noncoding RNAs in Alzheimer's disease. *Wiley Interdiscip Rev RNA* 2018; 9: 1463.
6. Ross SP, Baker KE, Fisher A, Hoff L, Pak ES, Murashov AK. MiRNA-431 prevents amyloid- β -induced synapse loss in neuronal cell culture model of Alzheimer's Disease by silencing Kremen1. *Front Cell Neurosci* 2018; 12: 87.
7. Zhao Y, Lukiw WJ. Microbiome-mediated upregulation of microRNA-146a in sporadic Alzheimer's Disease. *Front Neurol* 2018; 9: 145.
8. Meng YC, Ding ZY, Wang HQ, Ning LP, Wang C. Effect of microRNA-155 on angiogenesis after cerebral infarction of rats through AT1R/VEGFR2 pathway. *Asian Pac J Trop Med* 2015; 8: 829-835.
9. Zhao WJ, Zhang HF, Su JY. Downregulation of microRNA-195 promotes angiogenesis induced by cerebral infarction via targeting VEGFA. *Mol Med Rep* 2017; 16: 5434-5440.
10. Absalon S, Kochanek DM, Raghavan V, Krichevsky AM. MiR-26b upregulated in Alzheimer's Disease activates cell cycle entry, Tau phosphorylation, and apoptosis in post-mitotic neurons. *J Neurosci* 2013; 33: 14645-14659.
11. Jovicic A, Moser R, Santos MDFS, Silva Santos Mde F, Luthi-Carter R. MicroRNA-22 overexpression is neuroprotective via general anti-apoptotic effects and may also target specific Huntington's Disease-related mechanisms. *Plos One* 2013; 8: 54222.
12. Gunn-Moore D, Kaidanovich-Beilin O, Gallego-Irardi MC, Gunn-Moore F, Lovestone S. Alzheimer's disease in humans and other animals: A consequence of post-reproductive life span and longevity rather than aging. *Alzheimers Dement* 2018; 14: 195-204.
13. Segerstrom SC. Personality and incident Alzheimer's disease: Theory, evidence, and future directions. *J Gerontol* 2018; 12: 43.
14. Lu J, Shu R, Zhu Y. Dysregulation and dislocation of SFPQ disturbed DNA organization in Alzheimer's Disease and Frontotemporal Dementia. *J Alzheimers Dis* 2018; 22: 1311-1321.
15. Mnn V, Ras LF, DeFelice FG. Connecting Alzheimer's disease to diabetes: Underlying mechanisms and potential therapeutic targets. *Basic Clin Med* 2018; 136: 160-171.
16. An Y, Varma VR, Varma S, Casanova R, Dammer E, Pletnikova O. Evidence for brain glucose dysregulation in Alzheimer's disease. *Alzheimers Dement* 2018; 14: 318-329.
17. Kay DW. Genetics, Alzheimer's disease and senile dementia. *British J Psychiatr* 2018; 154: 311-320.
18. Hu X, Song C, Fang M, Li C. Simvastatin inhibits the apoptosis of hippocampal cells in a mouse model of Alzheimer's disease. *Exp Ther Med* 2018; 15: 1795-1802.
19. Gu C, Chen C, Wu R, Dong T, Hu X, Yao Y, et al. Long noncoding RNA EBF3-AS promotes neuron apoptosis in Alzheimer's Disease. *DNA Cell Biol* 2018; 37: 220-226.
20. Zhang Y, Wang J, Wang C, Li Z, Liu X, Zhang J, et al. Pharmacological basis for the use of Evodiamine in Alzheimer's Disease: Anti-oxidation and anti-apoptosis. *Int J Mol Sci* 2018; 19: 5.
21. Ting Y, Medina DJ, Strair RK, Schaar DG. Differentiation-associated miR-22 represses Max expression and inhibits cell cycle progression. *Biochem Biophys Res Commun* 2010; 394: 606-611.
22. Xu D, Takeshita F, Hino Y, Fukunaga S, Kudo Y, Tamaki A, et al. MiR-22 represses cancer progression by inducing cellular senescence. *J Cell Biol* 2011; 193: 409-424.
23. Song SJ, Ito K, Ala U, Kats L, Webster K, Sun SM, et al. The oncogenic microRNA (miR-22) targets the TET2 tumor suppressor

to promote hematopoietic stem cell self-renewal and transformation. *Cell Stem Cell* 2013; 13: 87-101.

24. Huang S, Wang S, Bian C, Yang Z, Zhou H, Zeng Y, et al. Upregulation of miR-22 promotes osteogenic differentiation and inhibits

adipogenic differentiation of human adipose tissue-derived mesenchymal stem cells by repressing HDAC6 protein expression. *Stem Cells Dev* 2012; 21: 2531-2540.